Journal of Manufacturing Processes 107 (2023) 240–251

Contents lists available at ScienceDirect

Journal of Manufacturing Processes

journal homepage: www.elsevier.com/locate/manpro

Investigation of surface integrity in grinding of nickel based superalloy under different cooling conditions

Dongdong Xu [a], Shusong Zan [b], Zhirong Liao [b,*], Yiqing Yang [c], Yukui Gao [d,*], Mingwang Fu [b,e]

[a] School of Mechanical Engineering, Tongji University, Shanghai, China
[b] Machining and Condition Monitoring Group, Faculty of Engineering, University of Nottingham, Nottingham, UK
[c] School of Mechanical Engineering, Beihang University, Beijing, China
[d] School of Materials Science and Engineering, Tongji University, Shanghai, China
[e] Department of Mechanical Engineering, Research Institute for Advanced Manufacturing, The Hong Kong Polytechnic University, Kowloon, Hung Hom, Hong Kong, China

ARTICLE INFO

Keywords:
Surface integrity
Grinding
Inconel 718
EBSD
Microhardness
Residual stress

ABSTRACT

While grinding has been employed as an important machining method to meet the workpiece quality requirement, the machined surface integrity of nickel based superalloy with/without coolants applied and under different cooling pressure has not been studied in detail regarding the subsurface microstructure and mechanical properties variation. This study gives a comprehensive investigation on the surface and subsurface characterization of workpieces machined with selected grinding conditions (dry, flood cooling and high pressure cooling), focusing on the in-depth exploration of the thermal influence on surface morphology generation, subsurface microstructure alteration, crystal orientation variation, and mechanical properties formation. The dry grinding process leads to significant subsurface material alternation in respect of both microstructure and mechanical properties. An obvious recrystallization and white layer are observed at the same time, which is an uncommon phenomenon in the former investigation of the ground surface. In addition, evident material soft is identified in the subsurface area of the workpiece acquired from the dry grinding scenario (hardness reduced to only half of the bulk materials in a large depth location). Interestingly, a plate-like η phase is observed inside the grains, which is influenced by the extreme thermal load. As a comparison, the introduced coolant not only improves the surface morphology (Ra value reduced 3.8 % and 13.2 % with flood cooling and high pressure cooling, respectively) but also alters the subsurface properties to a more industrial and machining preferable state. Smooth surface, no recrystallization, less hardness variation (microhardness variation depths are 1400 μm, 800 μm, and 600 μm under dry, flood cooling, high pressure cooling conditions, respectively), and compressive residual stress are obviously found from the present study. It is found that high pressure cooling can sufficiently carry away the grinding generated heat in time and deliver the coolant into the grinding region, which improves the ground workpiece quality. These findings could be of help for choosing suitable cooling methods in the industry and help understand the obtained part/components quality.

1. Introduction

Nickel based superalloys, classified as difficult-to-cut materials, have been widely used in safety critical areas such as aerospace, nuclear and medical sectors because of their excellent high temperature and corrosion resistance in extremely harsh working conditions [1–3]. However, when machining these kinds of materials, significant tool wear, poor surface integrity, and low material removal rates are quite common to be found [4,5], which makes it difficult to carry out high quality machining of nickel based superalloys. In addition, it is well-known that safety consideration is a priority in the above-mentioned application areas, thus the surface integrity of machined workpieces has been treated as one of the most important aspects to inspect the machined components.

Generally, grinding is used as the final machining process to achieve a higher geometry accuracy of the workpiece [6–9]. To improve the understanding of the performance of the grinding process, people have investigated the difference between micro-milling and grinding processes [10], reporting that the main difference is the randomness of the

* Corresponding authors.
E-mail addresses: zhirong.liao@nottingham.ac.uk (Z. Liao), yukuigao@tongji.edu.cn (Y. Gao).

https://doi.org/10.1016/j.jmapro.2023.10.027
Received 8 May 2023; Received in revised form 25 September 2023; Accepted 9 October 2023
Available online 24 October 2023

grit locations during the machining processes. Regarding the grinding process, it is reported that advance and innovation always relate to the increase of materials removal rate and decrease of ploughing. For example, the investigation of textured grinding wheels has reached the amounts of more than 15,000 papers. Most of them are focused on cutting edge distribution, protrusion, and orientation [11,12] to optimize the material removal process, as well as the effect of grit geometry on materials [13].

Because of the nature of the grinding process, the high temperature associated with the thermal effects of material is always found in the grinding region. It is well known that the temperature rises and excess is critical for the workpiece surface and subsurface generation. In grinding process, the high temperature will normally lead to an unfavorable surface burn, which can affect the performance of the workpiece. To reduce the grinding temperature and optimize the grinding process, coolants are commonly used for cooling and lubrication. It has been reported in literatures that not only does the chemical composition of fluids have an influence on the performance of the grinding process, but also their supply conditions play an important role in determining the grinding [14]. Because high fluid flow rates usually result in higher levels of pollution in the environment, it is necessary to investigate the method of reducing the applied fluid coolants and the influence of different cooling conditions on the workpiece [15,16]. Obviously, people have agreed and focused on the aim of employing grinding coolants being "as little as possible on the basis of as much as necessary" [17,18]. Apart from this, Philip investigated the influence of jet nozzle shape on coolant jet characteristics, its performance, as well as the generated gear profile [19]. Additionally, the effects of lubrication types (water or oil based ones) on the grinding process have been studied as well, e.g. commercial metal cutting fluids have been investigated [20].

Nevertheless, with the application of coolants in grinding, the surface integrity after machining has been altered [21–25] and this can affect the functional performance of components. For example, the fatigue performance can be affected by the micro cracks in recast layer; the corrosion resistance can be reduced due to the tensile residual stress on the surface; The wear resistance can be reduced due to lower hardness near the surface [26], etc. Although there are correlations between some aspects of surface integrity, e.g., the white layer formation can affect the microhardness near the surface [27,28], the relationship is not linear or other simple correlation. Based on this, it is necessary to evaluate from multiple aspects to obtain the comprehensive information of workpiece surface integrity. Because of the importance of machined surface integrity, researchers show great interest in carrying out the application of coolants on machined surface quality. Cryogenic cooling has been investigated for the machining process. It is mentioned that it works well for the turning process, but not in the grinding process, and only part of the subsurface materials were presented [29]. The surface integrity and fatigue performance of grinding are studied but coolants are not mentioned, while only surface morphology and residual stress are included in the research [30]. Kirsch et al. [31] studied the macro-topography of grinding wheels on the cooling efficiency and generated surface, but the context mainly talked about the grinding texture. Zhou et al. [32,33] carried out a simulation and experiment on the surface integrity of grail grinding, while the surface integrity aspects mainly refer to the surface topography and the subsurface deformation. Li et al. [34] studied the grinding with CBN wheels on powder metallurgy superalloy FGH96 and its surface integrity; similarly, only very rare surface integrity aspects such as surface roughness and subsurface material drag are presented.

Although the grinding processes and machined surfaces have been investigated by lots of researchers, most of the studies focus on the implementation of grinding, grinding tools improvement, grinding parameters combination, and the surface morphology after grinding. The detailed grinding surface integrity of nickel-based superalloys, including surface morphology, subsurface microstructure, deformation, and mechanical properties, have not been studied and compared together to reveal the mechanism that governs the surface integrity generation for grinding with wet or dry scenarios.

2. Aims and research concept

To understand the difference and reveal the generation mechanism of surface integrity in different grinding processes, this research investigates the nickel-based superalloy workpieces ground under dry conditions, with flood coolant, and with high-pressure cooling, focusing on the surface integrity characteristics in both surface and subsurface regions.

At first, the dry grinding process was carried out as the benchmark while grinding force was monitored during the process. As a comparison, two kinds of cooling, flood cooling (low pressure) and high-pressure cooling, were employed to present the difference in grinding results. Because of the different thermal and mechanical loadings (temperature, force, friction, etc.), various surface profiles and subsurface properties were evidently produced. The surface characteristics (e.g. roughness, profiles) were inspected to reveal the geometry accuracy and quality as well as the lubrication effects. The microstructure deformation influenced by the grinding temperature and force can be investigated by implementing the observation with material characterization techniques. Besides, the mechanical properties, such as microhardness, and residual stress are also measured by nanoindentation and XRD. To comprehensively discover the influence of different cooling processes on ground workpieces, the above-mentioned aspects were studied in detail and compared (Fig. 1).

3. Experimental methodology

In this investigation, the grinding tests are implemented on a modified grinding machine (Jones-Shipman 540P), and the Inconel 718 workpieces (dimension: 100 mm × 20 mm × 10 mm) are used for machining trials. Alumina grinding wheels (TYROLIT VU518562) with 150 mm diameter, 10 mm thickness, and 500 mesh is employed, and for each trial, the tool has been re-dressed by a diamond point dresser with 0.2 mm dressing parameter to avoid influence from tool wear. As illustrated in Fig. 2, the workpiece is fixed on a Kistler 9257BA dynamometer, which is used to acquire forces during the grinding process. Here, the dynamometer is clamped on the stage and moves with it to complete the grinding of the workpiece surface. Under each condition, three workpieces are ground and the force in the stable region (avoid the entering and exiting position) are used to calculate the average force in each process. Then the average value of three passes is calculated to represent the grinding force of each condition. A thermal camera is installed to monitor the grinding temperature for the dry grinding process (inaccessible for cooling conditions) as an indicator for understanding the subsurface microstructure variation. For the flood cooling process, the coolant (Hocut 3380) flows over of workpiece freely with no extra pressure. In high pressure cooling, the Chip Blaster Model CV26-3000 high pressure cooling system (see Fig. 2) is used and the coolant pressure is set as 1000 psi (69 bar, chosen based on the suggestion from the grinding wheel producer specially for turbine blade production). Under this pressure, a sufficient delivery of liquids into the grinding region can be achieved which can carry away the heat effectively. The adopted grinding parameter combination for different cooling conditions are grinding speed (3000 m/min), grinding depth (0.15 mm), grinding width (10 mm; grinding wheel thickness), and feed rate of 300 mm/min, which are shown in Table 1. In this research, aggressive grinding parameters are applied based on the requirement of the industrial partner. With these parameters, the deformation layers are clearer and can help understand the results of different cooling strategies under extreme conditions.

The machined surface of the workpiece has been studied by employing surface topography measurements (Alicona InfiniteFocus and MountsMap) at three random positions on the ground surface and

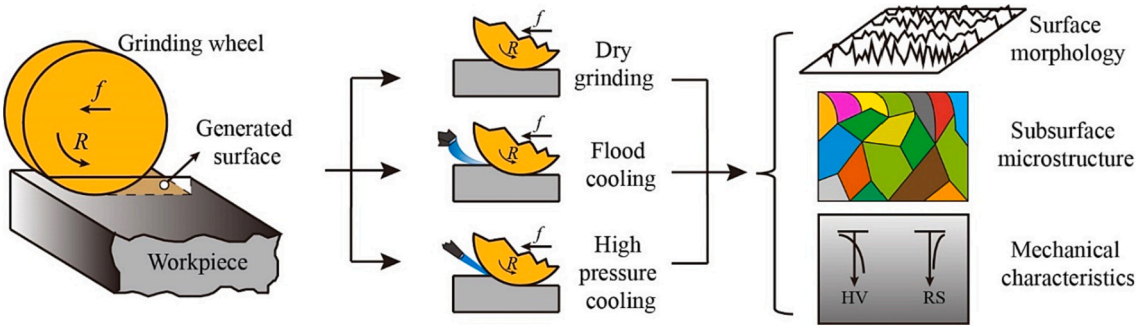

Fig. 1. Schematic of implemented grinding process with various cooling conditions.

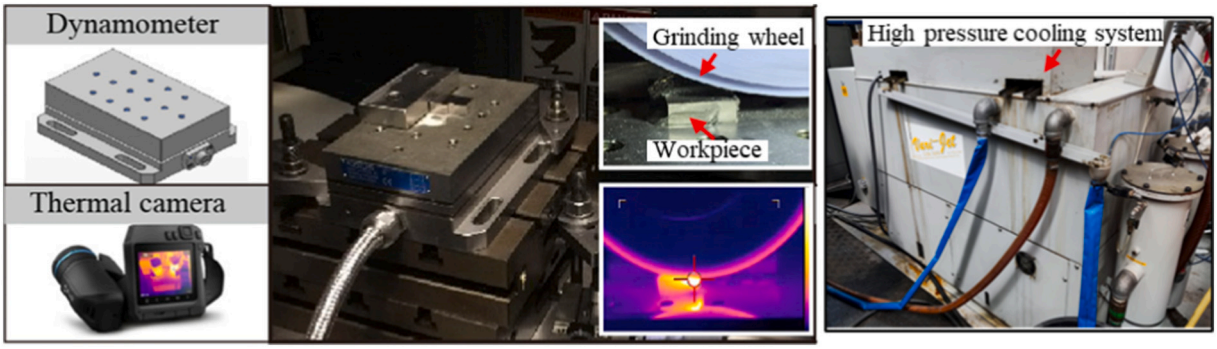

Fig. 2. Employed equipment for carrying out grinding investigation and corresponding monitoring accessories.

Table 1
Experimental parameters.

Speed	Feed rate	Grinding depth	Grinding width	Cooling pressure
3000 m/min	300 mm/min	0.15 mm	10 mm	0, 69 bar

High pressure cooling	Orifice Diameter	Velocity	Volume Flow rate	Stand-off distance
Values	0.15 mm	142 m/s	1.6 L/s	30 mm

the average value is used to evaluate the surface roughness. Samples of the workpieces for further analysis are prepared by mounting, grinding (SiC sandpaper P400, P800, P1200, and P4000 grit), and polishing (6 and 1 μm diamond suspension and 0.06 μm silica suspension). Scanning electron microscope (SEM, JEOL 7100F) and electron backscatter diffraction (EBSD, JEOL 7100F) were applied to investigate subsurface microstructure variation. A Proto iXRD machine was used to acquire the residual stress profile in the depth direction by employing a Mn tube and a 2 mm aperture. As another aspect of mechanical properties, the microhardness of the workpiece in the subsurface areas was tested with a nanoindentation instrument (NanoTest Vantage4) machine (target load 20 mN, dwell time 5 s).

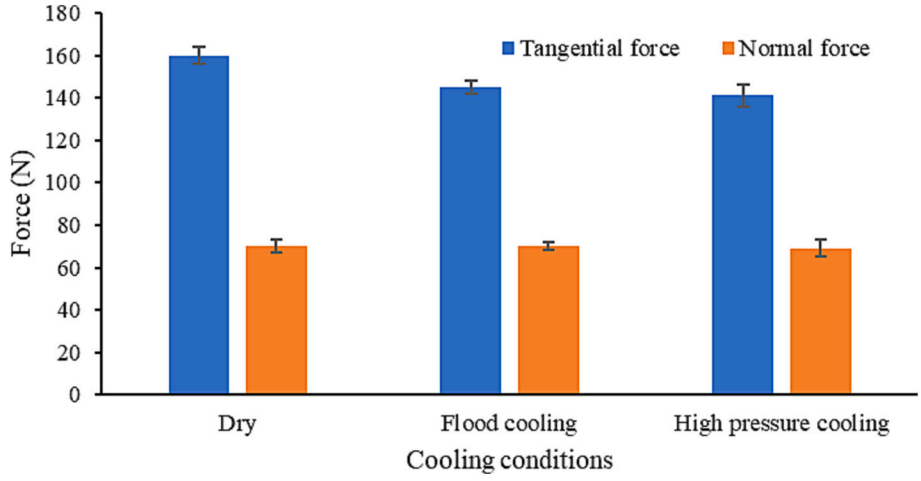

Fig. 3. Force under different cooling conditions.

4. Results and discussion

4.1. Mechanical grinding force

As one of the grinding process monitoring elements, the forces under different coolant conditions are presented in Fig. 3. For the dry condition, a force of 160 N in the tangential direction is found, while the force in wet conditions (both flood cooling and high pressure cooling) are slightly smaller (145 N 141 N, separately). If considering the measuring errors, the forces in flood cooling and high pressure cooling make no difference in both the tangential direction and normal direction. The larger force in tangential direction for dry condition (as indicated in Fig. 3) is attributed to lack of lubrication from coolant and the rapid tool wear caused by the high grinding temperature. Nevertheless, from the comparison of grinding forces in these conditions, it can be summarized that the supplying of coolant doesn't influence the grinding force significantly while the grinding temperature will be obviously reduced. But the lubrication will somehow play slightly roles on reducing the grinding force in tangential direction.

4.2. Surface characteristics of the workpiece

Although the surface texture tends to be used more as an index to present the tool wear, machine tool variation, etc. rather than to judge the performance of the machined workpieces, it is still a key indicator for evaluating the surface integrity, which has an important impact on the machining reliability of the workpiece. The surface roughness of machined workpieces in dry, flood cooling, and high pressure cooling are presented in Fig. 4. It can be seen that the dry grinding one shows the highest value (1.06 μm) meaning the worst surface roughness among these conditions, while the value is smaller (1.02 μm) when applying flood coolant and it decreases again (0.92 μm) after high pressure cooling is introduced. This is attributed to the fact that the high pressure coolant could be delivered to the cutting zone easily, which can reduce the temperature in that area and lubricate the contact between the tool and workpiece.

To provide greater insight into the surface finish, the three dimensional surface topography of workpieces presents the different peaks and valleys generated by grinding processes as seen in Fig. 5. Similar to the results of surface roughness, a more obvious peak distribution and surface irregularity can be seen for the workpiece acquired from dry grinding processes (Fig. 5a). The obvious peak microtexture on the surface indicates the intense interaction between grinding wheels and the surface in the dry grinding process, which causes the visible heavy surface smearing as well. As comparison, the surface topography for flood cooling condition generated workpiece is flatter with fewer peaks, meaning a better surface is acquired which can be seen from the above Sz value decrease (28.28 μm to 25.12 μm) as well. Furthermore, when high pressure cooling is used, the smallest surface peaks and valleys variation can be seen in Fig. 5c and f, implying the best surface generated by high pressure grinding in this investigation. The same phenomenon can be seen from the surface variation curves, in which the surface generated from the dry grinding process covers a wider band area, while it becomes narrow after flood cooling is introduced and decreases again in high pressure cooling. With no doubt, the cooling process will improve the surface quality when considering the surface topography to some extent, especially for the roughness. It has to be noted that the difference in roughness value is not large, showing that the cooling may not improve the roughness significantly.

4.3. Subsurface micro-structure investigation

The machined workpiece is sectioned and polished to inspect its subsurface microstructure, which is believed to have a tight relationship with its properties. As seen in Fig. 6, it shows a significant difference after the grinding process regarding the deformation layers and grain structures. For all of the workpieces, there is no obvious deformation noticed in the magnification of ×300 times (Fig. 6a, c, and e), but it has to be mentioned that the grain structures show differences after the same etching process. The grains acquired from the dry grinding process seem to have been fully etched and, for the samples under cooling conditions, both flood and high-pressure ones only show obvious etching marks in grain boundaries. This is clearer in the higher magnification images (×1000 times) that the inner structure of grains in Fig. 6b presents apparent very large precipitation, which is seen as a plate-like η phase [35] and this is believed to be influenced by the extremely high temperature in the dry grinding process. In contrast, there is no obvious η phase appearance under the cooling conditions and this is attributed to the lower temperature in the grinding process, which is not high enough to achieve the phase transformation. As we know that the microstructure variation will have an influence on its properties, this aspect is discussed in the latter microhardness results.

In respect of the subsurface deformation, a clear material drag can be noticed in the dry grinding process generated workpiece (Fig. 7a). Interestingly, at the top surface there is a clear white layer with a thickness of around 2 μm and beneath it, an "exotic layer" (6 μm,

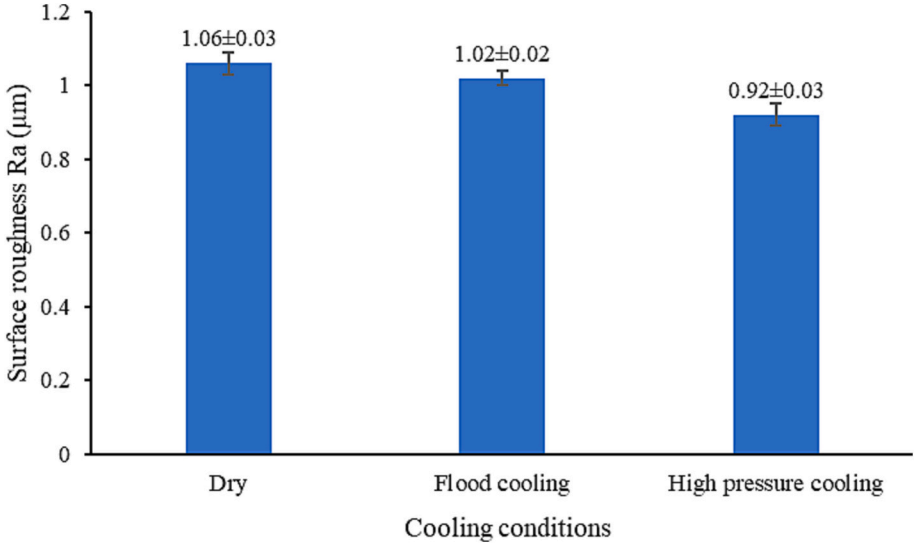

Fig. 4. Measured surface roughness of workpiece generated from dry, flood cooling, and high pressure cooling.

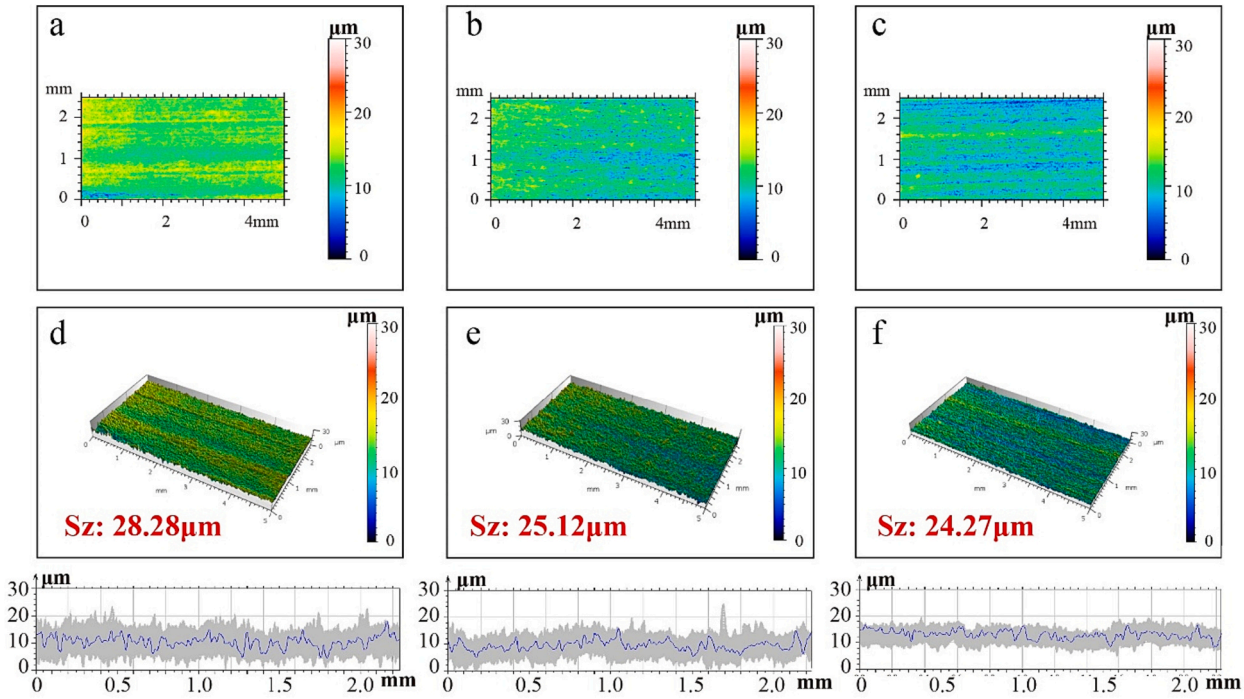

Fig. 5. The surface topography and profile acquired from the ground workpiece. Dry grinding processes- (a) and (d); flood cooling - (b) and (e); and high-pressure cooling – (c) and (f).

recrystallized grains as explained later) which is neither similar to the white layer nor to the bulk material is found and hasn't been reported before. Neighboring to the exotic layer, a clear material drag can be seen, indicated by the deformed η phase precipitation. These phenomena (enlarged view in Fig. 8) show that in this study not only the subsurface microstructure of the dry grinding process generated workpiece is very complex, but the depth of altered structure also approaches a depth of more than 10 μm. These microstructure alternations can reduce the fatigue endurance and affect the wear resistance of the workpiece [26]. As a comparison for the flood cooling, a deformation depth of 10 μm (material drag) can be found (Fig. 7b) with no white layer and "exotic layer". While considering the high pressure cooling generated workpiece there is only a plastic deformed layer that can be seen with non-obvious material drag and no white layer, presenting the best subsurface microstructure in the comparison study.

Moreover, to understand the subsurface microstructural variation in these three conditions, the microstructure characterization is carried out by employing EBSD measurement as shown in Fig. 9. Seen from Fig. 9a-ii, the white layer cannot be indexed can present as a black area at the top surface layer and this is correlated to the former observation in SEM images (Fig. 7a and Fig. 8). The neighboring area, presented as "exotic layer" in the SEM images, is obviously recrystallized grains because of the extremely high temperature (as indicated by the small grain layers in Fig. 9a-ii). This phenomenon is not common in the former investigation of the subsurface integrity of workpieces in the grinding process in literatures. Normally, a material drag layer is next to the white layer and no recrystallization layer is found. In addition, it is reported only in the investigation of a turning sample [36] that the grain recrystallization is found. But it is inside of the white layer, which is apparently different from this phenomenon. It presents that the recrystallization could be generated if the grinding process experienced a significant thermal influence under extensive harsh machining conditions. Because of the introducing of coolants, the grinding temperature is reduced. Thus no significant crystal recrystallization is observed in the latter two workpieces (flood cooling and high pressure cooling). For the flood cooling one (Fig. 9b), a slightly small grain layer at the edge can be seen (Fig. 9b-ii), while for the high pressure cooling one (Fig. 9c-ii) only heavy crystal deformation is found. Apart from the microstructure, the kernel average misorientation (KAM) map of inspected areas shows that remarkable misorientation has been imposed on the subsurface areas in the whole measured areas (Fig. 9a-iii) for the dry grinding process. The misorientation has been sharply decreased when the coolant is employed in the grinding processes although the flood coolant one still shows a more concentrated misorientation at the near surface area (Fig. 9b-iii) compared with the high pressure cooling generated one (Fig. 9c-iii). In addition, the EDS map of the subsurface area for different ground workpieces corresponding to the EBSD measured regions has also been acquired (Fig. 10); no exotic element and unusual chemical components are found, meaning that in these investigated grinding processes no significant chemical reaction is included.

These observed recrystallization and white layer have evidently emphasized the influence of temperature on subsurface microstructure alteration and have clarified the importance of carrying out different cooling measures.

To explore the properties of the superficial surface layer that are severely influenced by the machining process, the inverse pole figures of the near surface layer of the workpiece have been presented in Fig. 11. Obviously, for the area selected from the dry grinding process (Fig. 11a), no clear preferred orientation of grains have been found which can be evidenced by the phenomenon that no clear concentration is presented in the corresponding IPF figures (IPF in Fig. 11a) in three directions (X, Y, and Z). This is because, in the dry grinding process, the extremely high temperature has caused recrystallization in the layer below the white layer as shown in the former part, leading to random distribution of grain orientation in the newly generated small grain layer. Again, this result emphasizes the significant thermal influence in the dry grinding process. A relatively apparent orientation concentration can be seen in the Z direction in the IPF figure of Fig. 11b in respect of the workpiece generated from flood cooling conditions, while it is less obvious in the X and Y direction. The reason for this phenomenon is when flood cooling is employed, the temperature in the cutting zone and workpiece have been reduced a bit, but not enough to completely avoid the recrystallization of grains in the subsurface layer, thus a very slight layer of small grains can be seen and this have been proved by the EBSD results in Fig. 9.

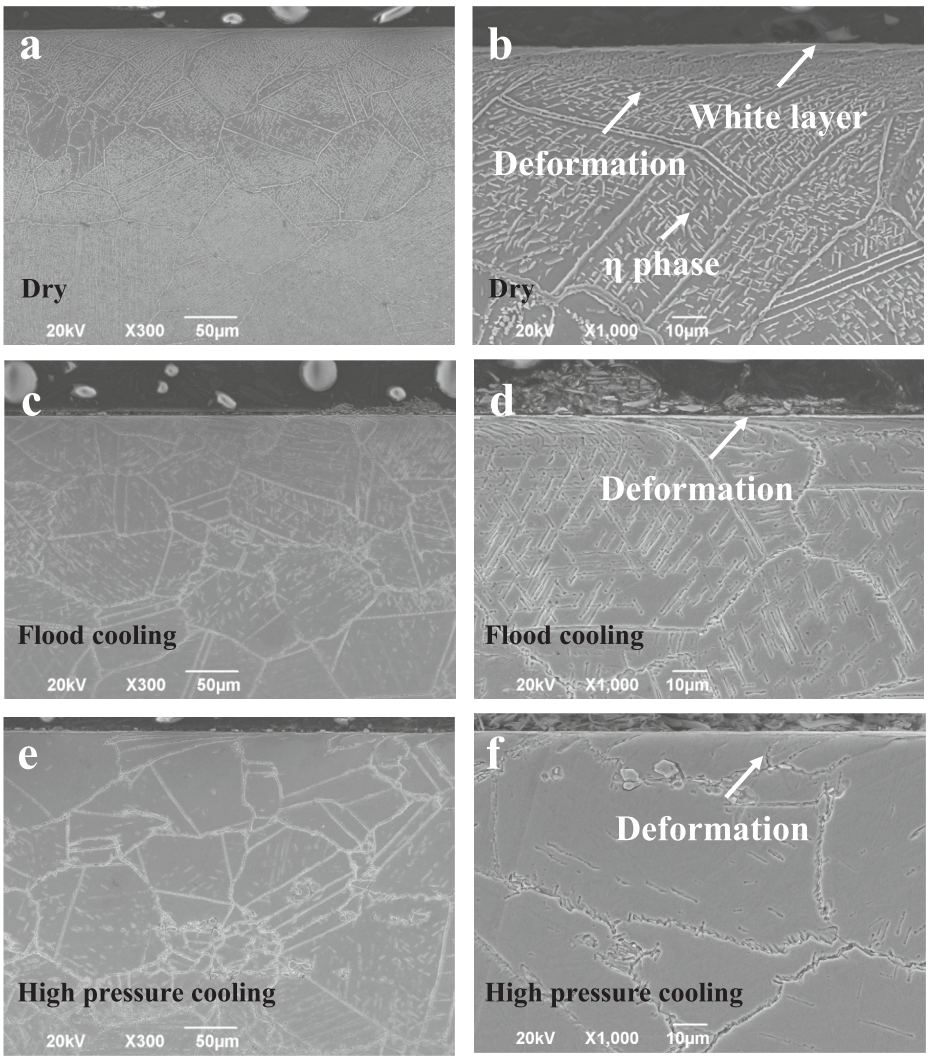

Fig. 6. SEM images of subsurface microstructure of workpiece in times of 300 and 1000 times. Dry grinding processes- (a) and (b); flood cooling - (c) and (d); and high-pressure cooling – (e) and (f).

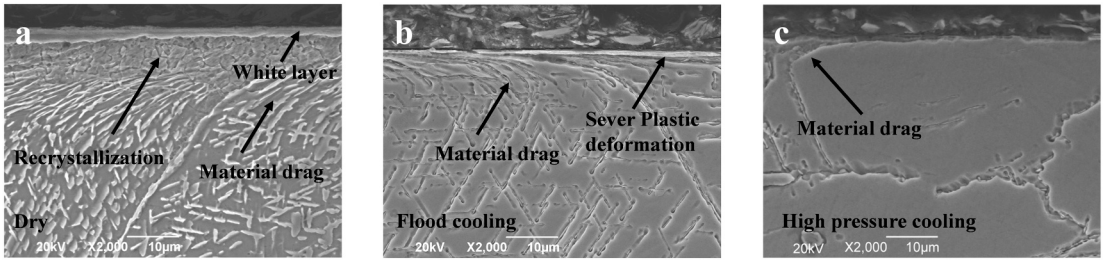

Fig. 7. SEM images of workpieces acquired from different grinding processes. Dry grinding processes-(a); flood cooling-(b); and high-pressure cooling-(c).

Because of this, the original grain expresses an orientation preferential in the Z direction, and the generated recrystallization layer leads to an average distribution at the other two directions. As anticipated, in the IPF figure of the workpiece acquired from high pressure cooling grinding process, an evident grain preferential orientation is observed from the IPF figure indicating that the grains in this layer are roughly in the same orientation. This is because in this scenario an appropriate cooling condition is achieved by employing high pressure cooling. Thus no recrystallization is generated and most of the grains maintain the original orientation or are slightly rotated, as the deformation that absolutely cannot lead to a significant orientation variation. These observed phenomena clarified the influence of cooling on subsurface grain orientation variation in the grinding process, keeping consistent with the former EBSD and SEM findings.

Furthermore, the point-to-point dislocation of the workpiece in the subsurface area, from surface to the depth direction (70 μm) and along the line in Fig. 12a, b, and c, has been analyzed to study the subsurface deformation. At first, it is worth noting that the misorientation larger than 50° in the area deeper than 15 μm is the original grain boundary in the bulk material. Regarding the dry grinding condition, several misorientations larger than 35° (peaks in a dark solid curve) are clearly observed in the depth of around 7 μm; this phenomenon is consistent

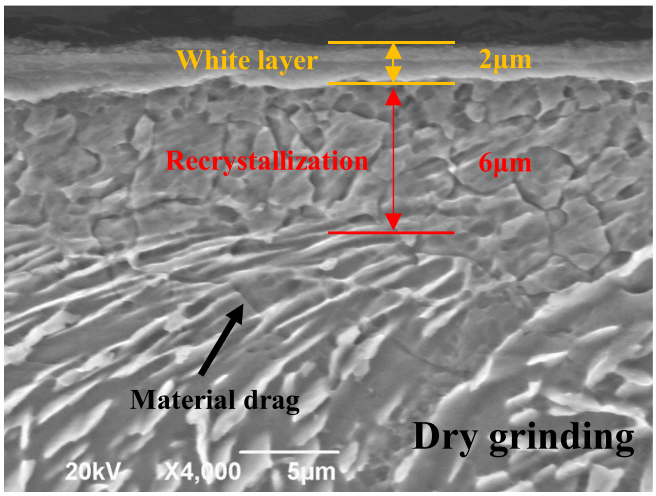

Fig. 8. Enlarged SEM images (4000 times) of the workpiece acquired from the dry grinding process to show the white layer, recrystallization, and material drag.

with the recrystallization layer as discussed (Fig. 12a), thus new grain boundaries are generated. As a comparison, for the sample acquired from flood cooling conditions (Fig. 12b), only one peak (larger than 20°) in the depth of 8 μm is found, corresponding with the thin recrystallized layer. However, considering the high-pressure cooling generated workpiece, a completely different phenomenon is presented that at the near surface area, a small misorientation of less than 20° can be seen, meaning that at this layer no recrystallization occurs but the deformation has caused the grain orientation variation. This keeps consistent with former SEM, EBSD, and IPF results that no crystallization but deformation is found in high-pressure cooling scenarios, proving the benefits of employing high pressure cooling in grinding.

4.4. Mechanical properties in the subsurface of the workpiece

It is well known that the work performance of a workpiece not only has a tight relationship with its surface topography and microstructure, but also affected by the mechanical properties. After experiencing the severe deformation and extreme temperature in grinding process, the microstructure on the machined surface varies, which is accompanied by the microhardness change as well. The curves of subsurface microhardness generated under different grinding conditions are presented in Fig. 13. Interestingly, an apparent microhardness decrease phenomenon

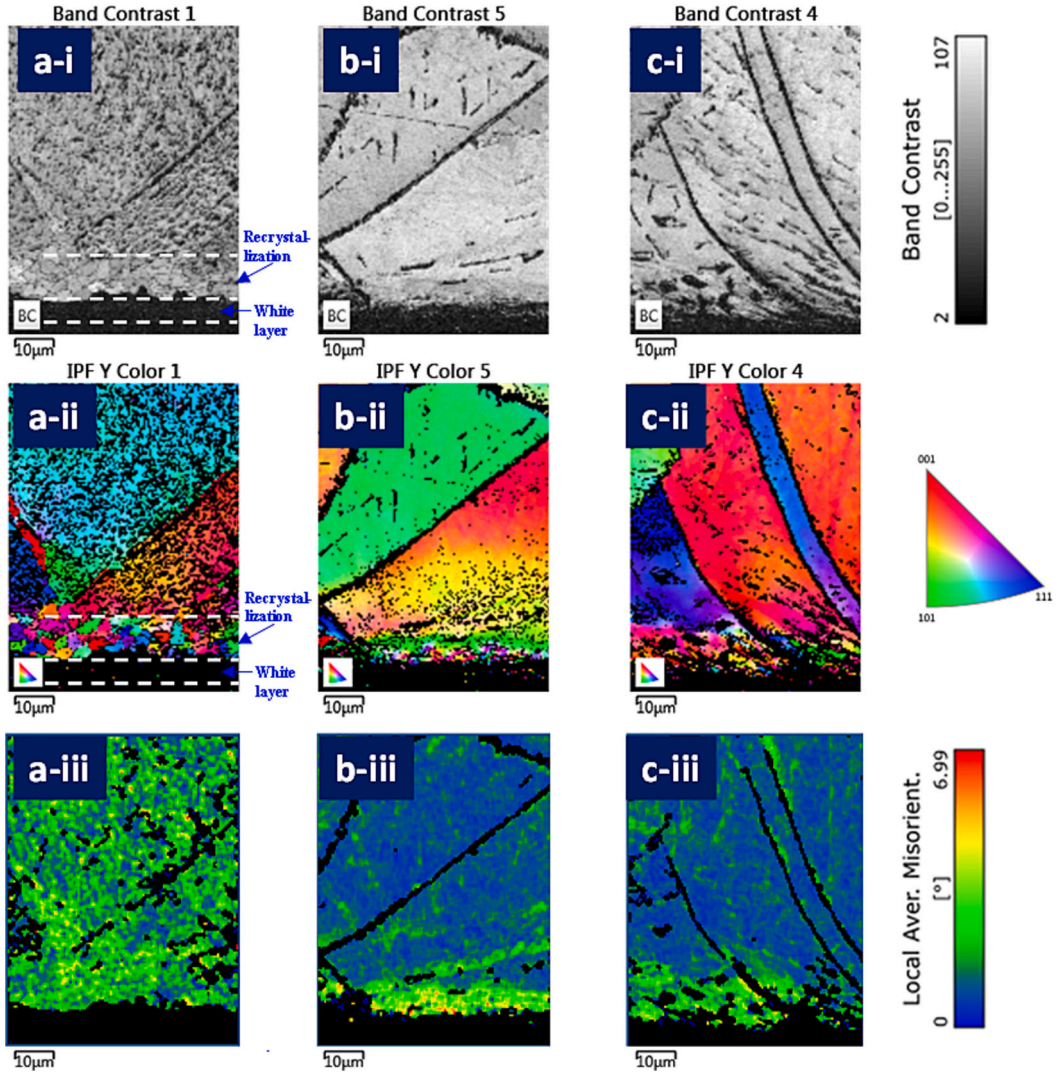

Fig. 9. The band contrast (i), inverse pole figure (IPF) (ii), and kernel average misorientation (KAM) map (iii) of subsurface area for different ground workpieces. Dry grinding processes-(a); flood cooling-(b); and high-pressure cooling-(c).

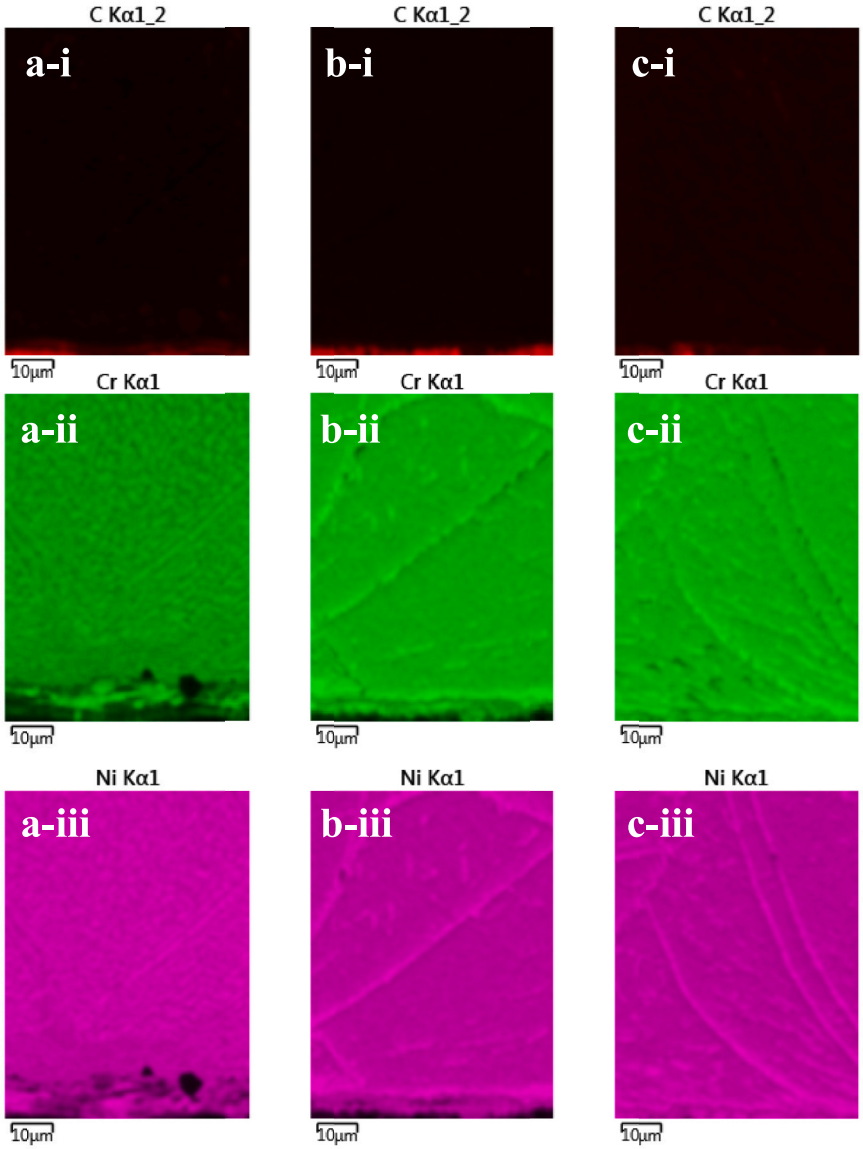

Fig. 10. Selected EDS map of the subsurface area for different ground workpieces corresponding to the EBSD measured regions. Dry grinding processes-(a); flood cooling-(b); and high-pressure cooling-(c).

is found for all of the grinding processes, which contradicts several published observations that the grinding-induced work-hardening leads to an increase in microhardness [37]. This can be explained by the fact that in the present investigation, the large grinding depth (150 μm) brings this grinding process into the extreme condition especially for the grinding temperature, even if the coolant is applied under the latter two conditions.

For the dry grinding process, the microhardness in the subsurface area has decreased to around 200–250 HV until the depth of 800 μm, and only at the depth of 1400 μm, the micro hardness value approaches back the bulk state (450 HV). This hardness reduction can reduce the corrosion resistance of the workpiece and affect the service life of components [26]. As a comparison, after the coolant is introduced for flood cooling, the subsurface soft phenomenon has been reduced significantly, showing a microhardness of 225 HV at 200 μm and becoming a bulk state at a depth of 600 μm. With no doubt, after high pressure cooling is employed, only the microhardness at a depth less than 150 μm is 225 HV and it has rapidly gone to around 400 HV at 200 μm and finally goes back to the bulk state before the depth approaching 400 μm. The comparison of subsurface microhardness for different grinding conditions is so evident, clearly presenting the significant difference before and after coolant is introduced and indicating the importance of carrying out high pressure cooling. Although the measurement depth of microhardness is much larger than the former microstructure results, they show the effect of grinding on these regions which can be further proved by the later residual stress results. Although the microstructure at large depth didn't show significant variation in former results, minor changes might be found by transmission electron microscope [38] and could be studied in further research. In addition, it shows that the extreme thermal influence will still alter the material microhardness beneath the surface when aggressive grinding parameters are used even if high pressure cooling is employed.

As known, thermal expansion and shrinkage, phase transformation, as well as plastic deformation, could lead to residual stress generation and variation [39]. While compressive residual stress are beneficial to component performance, tensile residual stress usually leads to crack formation and affect the corrosion resistance of workpiece [26]. In the present investigation, all the phase transformations, plastic deformation, and extreme thermal environments have been found in the grinding processes and discussed in detail. To reveal the residual stress

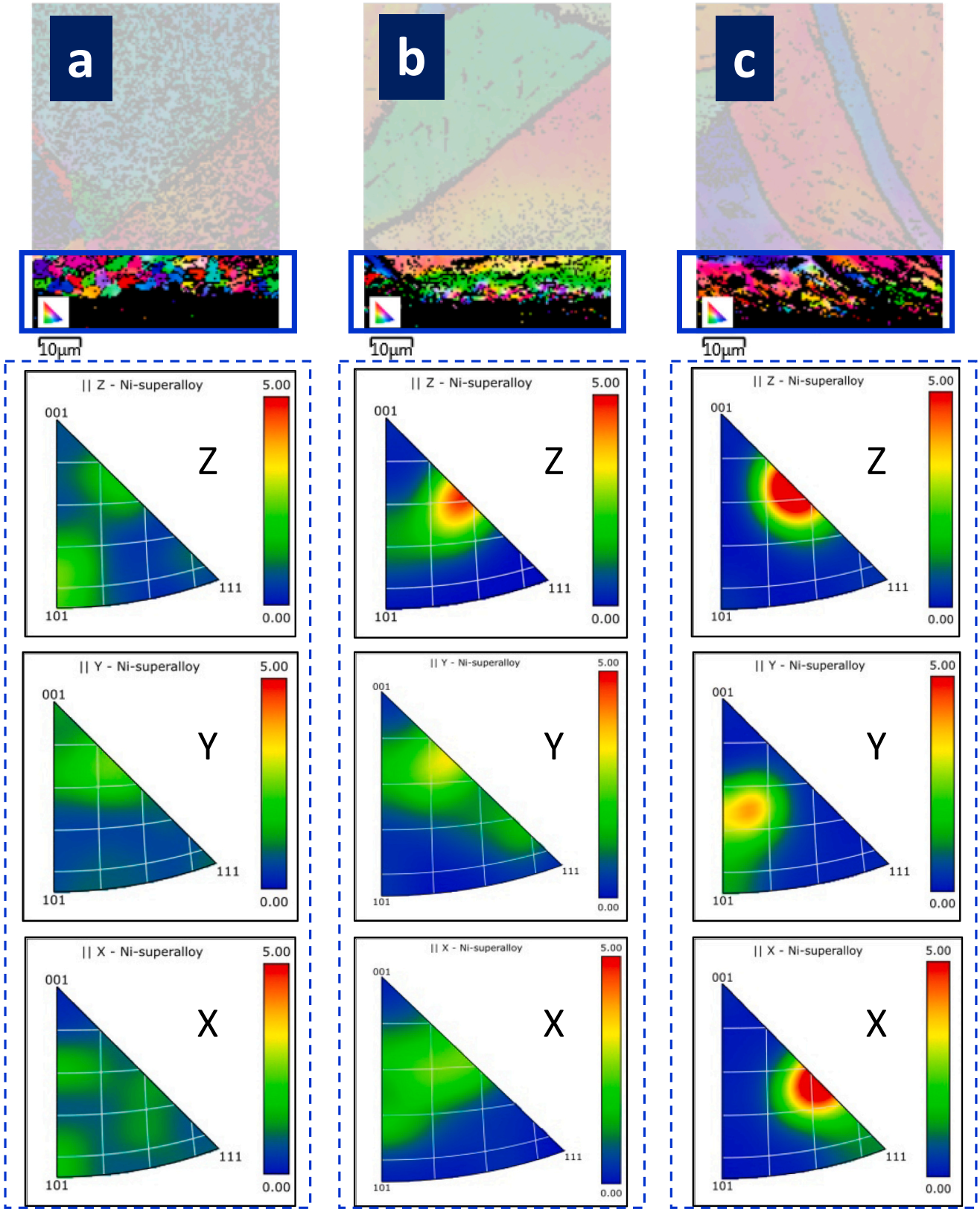

Fig. 11. Inverse pole figure (IPF) set of the selected near surface area of workpiece generated with different grinding conditions. Dry grinding processes-(a); flood cooling-(b); and high-pressure cooling-(c).

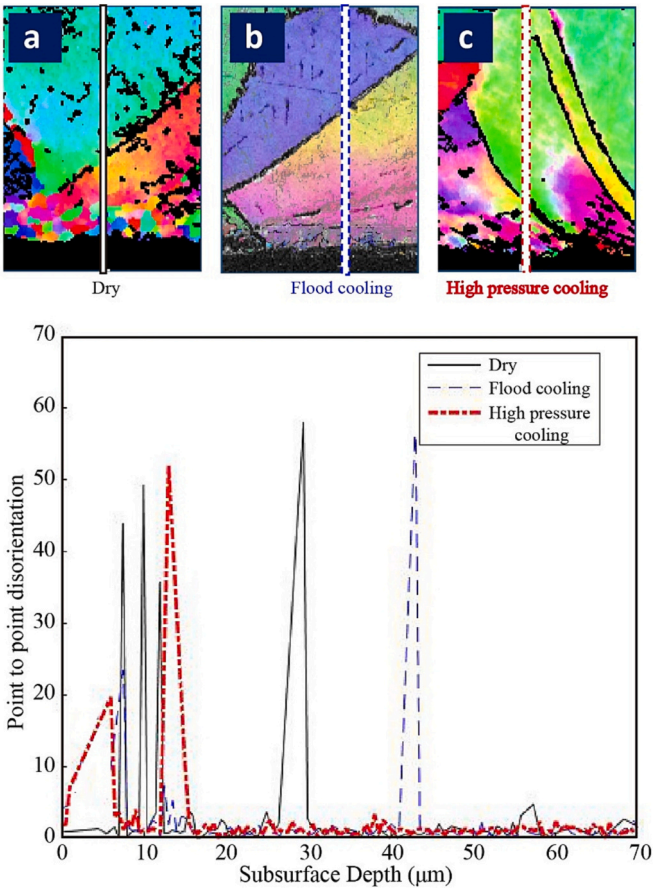

Fig. 12. Subsurface point-to-point dislocation of the workpiece in the depth direction from the surface to bulk areas. Dry grinding processes-(a); flood cooling-(b); and high-pressure cooling-(c); point-to-point curves for different workpieces-(d).

influenced by these aspects, the residual stress profile (Fig. 14) to the depth of 1500 μm from the surface has been acquired by removing the material layer by layer with electrical chemical polishing. The present residual stress is measured in the tangential direction while the orthogonal direction is neglected because theoretically, they should be similar in the distribution trend. Because of the high temperature and lack of cooling, the dry grinding process generates a workpiece with tensile stress (900 MPa) on the surface and it slowly decreases back to the level of bulk materials at the depth of around 1100 μm, while this is aligned with the observed thermal softening of the material. In the flood cooling condition, compressive stress is found on the surface and it turns to tensile stress quickly approaching 500 MPa at the depth of 150 μm before it goes back to a stable level at a depth of 400 μm. While the compressive stress is caused by the grinding generated plastic deformation (ploughing in the grinding process), as evidenced and agreed by literatures [40], the tensile stress in the deep area is obviously brought by the grinding temperature. The appearance of this phenomenon in the present test is because the extremely high temperature has a far deeper influence on the workpiece than the influence from grinding generated plastic deformation. This can be validated from the depth of plastic deformation in SEM and EBSD, while the thermal influence is indicated in the microhardness profile. Similarly, a high pressure cooling produces a workpiece with larger compressive residual stress (600 MPa on the surface) and a smaller peak tensile residual stress (200 MPa at a depth of 200 μm). Under this condition, a larger amount of heat has been taken away from high pressure cooling compared with flood cooling, thus the thermal influence on residual stress is reduced but the grinding caused plastic deformation almost keeps the same, leading to the observed residual stress profile (Fig. 14).

5. Conclusions

To reveal the surface integrity generation mechanism and the subsurface properties of the ground workpiece under dry, flood cooling and high pressure cooling conditions, the present study comprehensively investigates the grinding of Inconel 718 by particularly focusing on its surface morphology, subsurface microstructure, grain structure

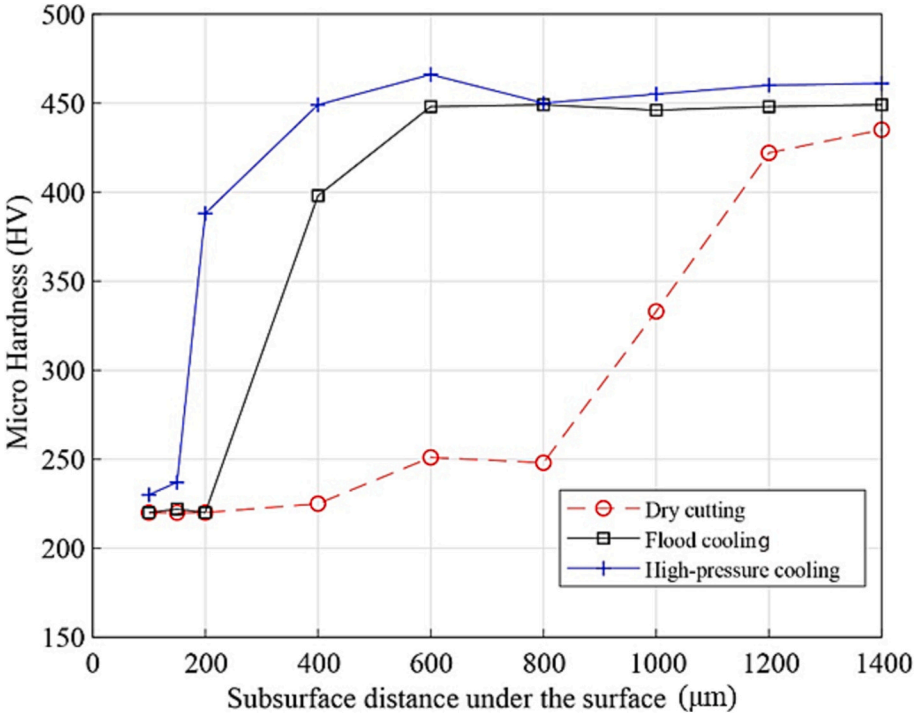

Fig. 13. Subsurface microhardness profile as a function of depth for workpiece acquired from different grinding conditions.

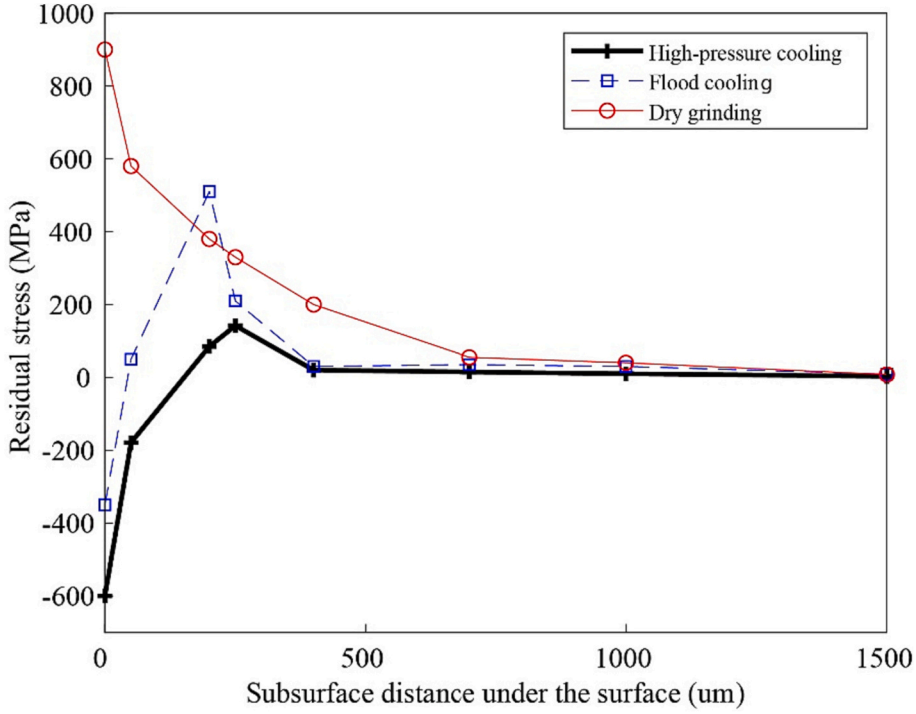

Fig. 14. Subsurface residual stress profile of workpiece acquired from different grinding conditions.

alternation, microhardness, residual stress, etc. The main finding of the present investigation can be summarized as follows:

1) The employing of coolants did not significantly alter the grinding force and generated surface morphology. The measured surface topography only shows that the surface roughness values (Ra) slightly decrease in flood condition (reduced 3.8 %) and high-pressure condition (reduced 13.2 %) compared to dry condition.
2) The extremely high temperature in dry grinding leads to the generation of an obvious thick white layer and recrystallization layer under it. In the area influenced by the extreme thermal load, a plate-like η phase appeared inside the grains. While under flood and high pressure cooling conditions, the white layer and recrystallization has been almost eliminated, showing the influence of applying coolants on subsurface microstructure formation.
3) The details of the subsurface microstructure variation are checked by EBSD results. The recrystallization under the white layer in the dry grinding process is clearly presented, but no chemical or exotic elements are found in it. While for both cooling conditions, the orientation preferential distribution of near surface grains and the point-to-point curves along the depth direction further proves the missing of white layer and recrystallization.
4) The microhardness and residual stress profile from surface to bulk material shows interesting phenomena. Under the dry grinding condition, not only high tensile residual stress (900 MPa) is observed in the surface and depth of 1000 μm, but the nano hardness decreases to only half (225 HV) of the bulk material (450 HV). When coolant is introduced, the soft phenomena have been largely reduced (microhardness variation depths are 800 μm, and 600 μm under flood cooling and high pressure cooling conditions, respectively, compared to 1400 μm under dry conditions) and the high pressure one shows better performance in both affected depth and absolute values of residual stress and microhardness.

All of the findings prove the benefits of employing high pressure cooling in grinding, which can help improve the obtained workpiece quality. In the future, the functional performance (e.g., fatigue, wear) of the workpiece acquired from these conditions is worth to be investigated for further understanding of the relationships among surface integrity results and practical service performance.

Declaration of competing interest

The authors declare that they have no known competing financial interests or personal relationships that could have appeared to influence the work reported in this paper.

Acknowledgment

This project has received funding from the National Natural Science Foundation of China (52205493), Shanghai Pujiang Program (21PJD072), the MARIE SKŁODOWSKA-CURIE ACTIONS (H2020-MSCA-COFUND-2014): The Integration of Novel Aerospace Technologies “INNOVATIVE” (No: 665468), Royal Society International Exchanges 2022 Cost Share (NSFC) (IEC\NSFC\223168) and Royal Society Wolfson Visiting Fellowships 2022 Round 2 (RSWVF\R2\222005).

References

[1] Chamanfar A, Sarrat L, Jahazi M, Asadi M, Weck A, Koul AK. Microstructural characteristics of forged and heat treated Inconel-718 disks. Mater Des 2013;52:791–800. https://doi.org/10.1016/j.matdes.2013.06.004.
[2] Liao Z, Axinte D, Mieszala M, M'Saoubi R, Michler J, Hardy M. On the influence of gamma prime upon machining of advanced nickel based superalloy. CIRP Annals 2018;67:109–12. https://doi.org/10.1016/j.cirp.2018.03.021.
[3] Lin YC, Li K-K, Li H-B, Chen J, Chen X-M, Wen D-X. New constitutive model for high-temperature deformation behavior of inconel 718 superalloy. Mater Des 2015;74:108–18. https://doi.org/10.1016/j.matdes.2015.03.001.
[4] la Monaca A, Axinte DA, Liao Z, M'Saoubi R, Hardy MC. Towards understanding the thermal history of microstructural surface deformation when cutting a next generation powder metallurgy nickel-base superalloy. Int J Mach Tool Manuf 2021;168:103765. https://doi.org/10.1016/j.ijmachtools.2021.103765.
[5] Wang B, Liu Z, Cai Y, Luo X, Ma H, Song Q, et al. Advancements in material removal mechanism and surface integrity of high speed metal cutting: a review. Int J Mach Tool Manuf 2021;166:103744. https://doi.org/10.1016/j.ijmachtools.2021.103744.
[6] Rowe WB. Principles of modern grinding technology. 2nd ed. William Andrew; 2013.

[7] Chen X, Morgan MN. Advances in quality and productivity in precision grinding-a review of selected research. In: ASME 2016 11th international manufacturing science and engineering conference, MSEC 2016. 1; 2016. p. 1–10. https://doi.org/10.1115/MSEC20168585.
[8] Guo S, Lu S, Zhang B, Cheung CF. Surface integrity and material removal mechanisms in high-speed grinding of Al/SiCp metal matrix composites. Int J Mach Tool Manuf 2022;178:103906. https://doi.org/10.1016/j.ijmachtools.2022.103906.
[9] Macerol N, Franca LFP, Drazumeric R, Krajnik P. The effects of grit properties and dressing on grinding mechanics and wheel performance: analytical assessment framework. Int J Mach Tool Manuf 2022;180:103919. https://doi.org/10.1016/j.ijmachtools.2022.103919.
[10] Shore P, Morantz P, Luo X, Tonnellier X, Collins R, Roberts A, et al. Big OptiX ultra precision grinding/measuring system, Jena, Germany. 2005. p. 59650Q. https://doi.org/10.1117/12.624166.
[11] Malkin S, Guo C. Grinding technology: theory and application of machining with abrasives. Industrial Press Inc.; 2008.
[12] Rowe WB. Principles of modern grinding technology. William Andrew; 2013.
[13] Zhang Y, Zhu S, Zhao Y, Yin Y. A material point method based investigation on crack classification and transformation induced by grit geometry during scratching silicon carbide. Int J Mach Tool Manuf 2022;177:103884. https://doi.org/10.1016/j.ijmachtools.2022.103884.
[14] Rowe B. Modern grinding technology and systems. MDPI; 2019.
[15] Jackson MJ, Mills B. Interfacial bonding between corundum and glass. J Mater Sci Lett 2000;19:915–7.
[16] Majumdar S, Das P, Kumar S, Roy D, Chakraborty S. Evaluation of cutting fluid application in surface grinding. Measurement 2021;169:108464. https://doi.org/10.1016/j.measurement.2020.108464.
[17] Kirsch B. The impact of contact zone flow rate and bulk cooling on the cooling efficiency in grinding applying different nozzle designs and grinding wheel textures. CIRP J Manuf Sci Technol 2017;18:179–87.
[18] Webster J, Brinksmeier E, Heinzel C, Wittmann M, Thoens K. Assessment of grinding fluid effectiveness in continuous-dress creep feed grinding. CIRP Ann 2002;51:235–40.
[19] Geilert P, Heinzel C, Wagner A. Grinding fluid jet characteristics and their effect on a gear profile grinding process. Inventions 2017;2:27.
[20] Arrabiyeh PA, Bohley M, Ströer F, Kirsch B, Seewig J, Aurich JC. Experimental analysis for the use of sodium dodecyl sulfate as a soluble metal cutting fluid for micromachining with electroless-plated micropencil grinding tools. Inventions 2017;2:29.
[21] Brinksmeier E, Heinzel C, Wittmann M. Friction, cooling and lubrication in grinding. Cirp Ann 1999;48:581–98.
[22] Nadolny K. Small-dimensional sandwich grinding wheels with a centrifugal coolant provision system for traverse internal cylindrical grinding of steel 100Cr6. J Clean Prod 2015;93:354–63.
[23] de Oliveira JFG, da Silva EJ, Guo C, Hashimoto F. Industrial challenges in grinding. CIRP Ann 2009;58:663–80.
[24] Malkin S. Current trends in CBN grinding technology. CIRP Ann 1985;34:557–63.
[25] Rowe WB, Black SCE, Mills B, Qi HS, Morgan MN. Experimental investigation of heat transfer in grinding. CIRP Ann 1995;44:329–32.
[26] la Monaca A, Murray JW, Liao Z, Speidel A, Robles-Linares JA, Axinte DA, et al. Surface integrity in metal machining - part II: functional performance. Int J Mach Tool Manuf 2021;164:103718. https://doi.org/10.1016/j.ijmachtools.2021.103718.
[27] Liao Z, La Monaca A, Murray J, Speidel A, Ushmaev D, Clare A, et al. Surface integrity in metal machining - part I: fundamentals of surface characteristics and formation mechanisms. Int J Mach Tool Manuf 2021;162:103687. https://doi.org/10.1016/j.ijmachtools.2020.103687.
[28] Axinte D, Huang H, Yan J, Liao Z. What micro-mechanical testing can reveal about machining processes. Int J Mach Tool Manuf 2022;183:103964. https://doi.org/10.1016/j.ijmachtools.2022.103964.
[29] Chaabani S, Arrazola PJ, Ayed Y, Madariaga A, Tidu A, Germain G. Comparison between cryogenic coolants effect on tool wear and surface integrity in finishing turning of Inconel 718. J Mater Process Technol 2020;285:116780.
[30] Xiao G, Chen B, Li S, Zhuo X, Zhao Z. Surface integrity and fatigue performance of GH4169 superalloy using abrasive belt grinding. Eng Fail Anal 2022;142:106764.
[31] Kirsch B, Aurich JC. Influence of the macro-topography of grinding wheels on the cooling efficiency and the surface integrity. Proc CIRP 2014;13:8–12.
[32] Zhou K, Ding H, Wang W, Guo J, Liu Q. Surface integrity during rail grinding under wet conditions: full-scale experiment and multi-grain grinding simulation. Tribol Int 2022;165:107327. https://doi.org/10.1016/j.triboint.2021.107327.
[33] Vignesh R, Arunachalam N. Design and development of spiral grooved grinding wheel and their influence on the performance of vertical surface grinding process. Proc Manuf 2021;53:251–9.
[34] Ziming W, Haining W, Xun L, Yu J, Rufeng X. Surface integrity of powder metallurgy superalloy FGH96 affected by grinding with electroplated CBN wheel. Proc CIRP 2020;87:204–9.
[35] Gianfrancesco AD. Materials for ultra-supercritical and advanced ultra-supercritical power plants. Woodhead Publishing; 2016.
[36] Liao Z, Polyakov M, Diaz OG, Axinte D, Mohanty G, Maeder X, et al. Grain refinement mechanism of nickel-based superalloy by severe plastic deformation - mechanical machining case. Acta Mater 2019;180:2–14. https://doi.org/10.1016/j.actamat.2019.08.059.
[37] Peng R, He X, Tong J, Tang X, Wu Y. Application of a tailored eco-friendly nanofluid in pressurized internal-cooling grinding of Inconel 718. J Clean Prod 2021;278:123498.
[38] Slama C, Abdellaoui M. Structural characterization of the aged Inconel 718. J Alloys Compd 2000;306:277–84. https://doi.org/10.1016/S0925-8388(00)00789-1.
[39] Ding C, Li X, Zhu H-Y, Chen F-W, Li F, Chang H. Microstructure evolution and phase transformation kinetics of low cost Ti-35421 titanium alloy during continuous heating. J Mater Res Technol 2021;14:620–30.
[40] Yao CF, Jin QC, Huang XC, Wu DX, Ren JX, Zhang DH. Research on surface integrity of grinding Inconel718. Int J Adv Manuf Technol 2013;65:1019–30.